frontiers | Frontiers in Energy Research

TYPE Original Research
PUBLISHED 17 August 2022
DOI 10.3389/fenrg.2022.935648

OPEN ACCESS

EDITED BY
Shripad T. Revankar,
Purdue University, United States

REVIEWED BY
Gerardo Maria Mauro,
University of Sannio, Italy
Jiankai Yu,
Massachusetts Institute of Technology,
United States

*CORRESPONDENCE
Bin Liu,
liubin871204@126.com
Yi Tan,
sharpty@sina.com
Guang Hu,
guanghu@mail.xjtu.cn

SPECIALTY SECTION
This article was submitted to Nuclear Energy,
a section of the journal
Frontiers in Energy Research

RECEIVED 04 May 2022
ACCEPTED 21 July 2022
PUBLISHED 17 August 2022

CITATION
Liu B, Tan Y, Jing F, Hu G and Yan M (2022), Study on multi-objective optimization for nuclear reactor radiation shield design coupling genetic algorithm with paralleling discrete ordinate code.
Front. Energy Res. 10:935648.
doi: 10.3389/fenrg.2022.935648

Study on multi-objective optimization for nuclear reactor radiation shield design coupling genetic algorithm with paralleling discrete ordinate code

Bin Liu[1]*, Yi Tan[1]*, Futing Jing[1], Guang Hu[2]* and Mingfei Yan[3]

[1]Science and Technology on Reactor System Design Technology Laboratory, Nuclear Power Institute of China, Chengdu, China, [2]School of Nuclear Science and Technology, Xi'an Jiaotong University, Xi'an, Shannxi, China, [3]RIKEN Center for Advanced Photonics, RIKEN, Wako, Saitama, Japan

An optimization method combining a genetic algorithm and the paralleling discrete ordinate code is developed and applied to the shielding design of the Savannah reactor. Several approaches are studied to cope with the multi-objective optimization problem, such as transforming into single-objective optimization approach, non-dominated sorting approach, and the approach of adding constraints on sub-objectives. Comparing with the current design methods, the optimization method developed in this study shows better performance since the discrete ordinate calculations are free of statistical fluctuations. The multi-objective optimization approach with constraints on sub-objectives seems to have the best performance. More optimized individuals satisfying the constraints can be obtained, and the optimized objectives show the best improvements comparing with the initial design.

KEYWORDS

multi-objective optimization, genetic algorithm, Pareto optimality, paralleling SN code, nuclear reactor shielding

1 Introduction

The radiation shielding design is of great significance for high-performance advanced nuclear reactors, such as nuclear marine propulsion systems (Yamaji and Sako, 1994), space reactors, and some other advanced nuclear systems (El-Genket, 2009). The primary purpose of the radiation shielding design is to design a shield enclosing the nuclear reactor to attenuate radiations and make the radiation dose out of the shield as low as reasonably achievable (ALARA) (Chen et al., 2019). Meanwhile, for those nuclear reactors in which space is limited, the shield also needs to be compact, light-weighted, and maybe specialized. As a result, the radiation shielding design problem can be modeled as a multi-objective optimization problem, given by

$$\text{minimize } f\left(\vec{x}\right) = \left[f_1\left(\vec{x}\right), f_2\left(\vec{x}\right), \cdots, f_m\left(\vec{x}\right)\right]^T$$
$$\text{subject to} \begin{cases} f_i\left(\vec{x}\right) \le f_{i,0}, i = 1, 2, \cdots, m \\ \text{subject to} \begin{cases} \vec{x} = (x_1, x_2, \cdots, x_n), x \in R^n \\ L_j \le x_j \le U_j, \left(j = 1, 2, \cdots, n\right) \\ h_k\left(x_j\right) \le 0, \left(k = 1, 2, \cdots, q\right) \\ v_l\left(x_j\right) = 0, \left(l = 1, 2, \cdots, p\right) \end{cases} \end{cases} \quad (1)$$

where $\vec{x}$ is a n-dimensional variable vector of the design parameters; $f_i(\vec{x})$ represents the sub-objective of the optimization; $f_{i,0}$ represents the tolerable limit of the sub-objectives; the values L_j and U_j represent the lower and upper bounds of the variables, respectively; and the inequality and equality equations h_k and v_l represent some domain constraints for the parameters considering the economical or engineering conditions.

Conventionally, the radiation shielding structures are designed through trial-and-error procedure (Cacuci, 2010; Cai et al., 2018; Ahmad et al., 2021), which performs as follows: first, an initial shielding design is proposed according to the designer's expertise; then the initial design is modeled and simulated with radiation transportation codes, such as Monte Carlo codes and SN (discrete ordinate) codes. Second, design objectives are analyzed. If the required objectives are not satisfied, the parameters of the shielding structure are modified according to the designer's experience, and another solution is obtained, simulated, and analyzed. The conventional method is time-consuming, has low efficiency, and the optimal solution is always hard to obtain. In recent years, multi-objective optimization algorithms are introduced into the shielding design field. Tunes et al. (2017) combine the Matlab (Matrix Laboratory) optimization toolbox with MCNP (A General Monte Carlo N-Particle Transport Code) to optimize the biological shielding structure of a compact pressurized water nuclear reactor. Chen et al. developed the optimization method combining a non-dominated sorting algorithm with the Monte Carlo code MCNP, which is applied to the shielding design of the Savannah reactor (Chen et al., 2019; Chen et al., 2020). Wu et al. (2021) combined the PSO (Particle Swarm Optimization) multi-objective optimization algorithm with the one-dimensional SN code ANISN (A One-Dimensional Discrete Ordinates Transport Code with Anisotropic Scattering) to optimize the nuclear reactor shielding structure. In addition, the optimization methods combining multi-objective optimization algorithms with radiation transportation codes are also used to the shielding design of the accelerator-driven neutron source (Ma et al., 2021).

As is stated previously, the current multi-objective optimization methods of shielding design mainly combine multi-objective algorithms with radiation transportation codes. The non-dominated sorting algorithm is the most widely used algorithm for multi-objective optimization. Two main drawbacks exist among the current optimization methods. First, constraints of the sub-objectives are not added, so normally there are solutions of which the sub-objectives are beyond tolerable limits. In addition, the commonly used radiation transportation codes are the Monte Carlo code and one-dimensional SN code. Simulations of Monte Carlo codes are always fluctuated as a result of its statistical nature (Zhuang, et al., 2019), causing difficulty for the optimization algorithms in searching for global optimal solutions. Also, the one-dimensional SN code cannot simulate the real radiation transportation problems.

In this study, an optimization design method for the nuclear reactor radiation shielding structure is developed. The non-dominated sorting algorithm is used for multi-objective optimization. Constraints of the sub-objectives are added to ensure sub-objectives of the optimized solutions within tolerable limits. In addition, the paralleling three-dimensional SN code *Hydra* is used to perform the radiation transportation calculations. *Hydra* was developed by the NECP (Nuclear Engineering Computational Physics) laboratory which uses the Koch–Baker–Alcouffe (KBA) algorithm to perform the parallelization calculation (Wang et al., 2020). The aim of this study is to develop an accurate and efficient optimization method solving the multi-objective optimization problem of the nuclear reactor shielding design, with the optimized solutions of which sub-objectives are within the tolerable limits.

2 Methodology

Based on the optimization method, combining genetic algorithms with the paralleling SN code *Hydra*, several approaches are studied for the multi-objective optimization problem stated by Eq. 1, which are illustrated as follows.

2.1 Approach 1: The single-objective method

This approach converts the multi-objective optimization problem into a single-objective optimization problem by setting the other sub-objectives as constraints, given as

$$\text{minimize } f\left(\vec{x}\right) = \left[f_i\left(\vec{x}\right)\right]^T, i = 1, 2, \cdots, m$$
$$\text{subject to} \begin{cases} f_i\left(\vec{x}\right) \le f_{i,0}, j = 1, 2, \cdots, m;\ j \ne i \\ \text{subject to} \begin{cases} \vec{x} = (x_1, x_2, \cdots, x_n), x \in R^n \\ L_j \le x_j \le U_j, \left(j = 1, 2, \cdots, n\right) \\ h_k\left(x_j\right) \le 0, \left(k = 1, 2, \cdots, q\right) \\ v_l\left(x_j\right) = 0, \left(l = 1, 2, \cdots, p\right) \end{cases} \end{cases} \quad (2)$$

In order to eliminate the individuals not satisfying the constraints, the subobjectives are transformed by,

10.3389/fenrg.2022.935648

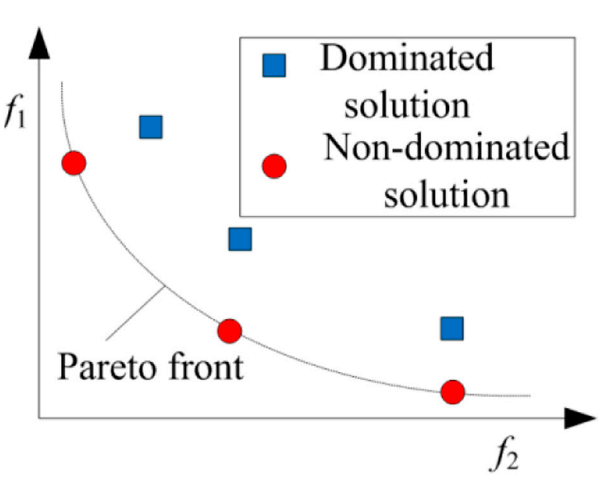

FIGURE 1
Pareto front of the two-objective-minimization problem.

$$g_i(\vec{x}) = \begin{cases} \dfrac{1}{1+f_i(\vec{x})}, & if\ f_i(\vec{x}) \le f_{i,0}(\vec{x}) \\ 0 & else \end{cases} \tag{3}$$

Thus, the minimization problem stated by Eq. 2 can be transformed into the maximization problem given by

$$\text{maximize } g(\vec{x}) = \left[g_i(\vec{x})\right]^T. \tag{4}$$

As a result, the multi-objective minimization problem of the shielding design is converted into a single-objective maximization problem by treating the individuals not satisfying the constraints as "lethal genes", of which the fitness values are set to be 0. A single-objective genetic algorithm based on elitism is applied to solve the single-objective maximization problem stated by Eq. 4 (Zhou and Sun, 1999).

2.2 Approach 2: The non-dominated sorting method

In most cases, sub-objectives of the multi-objective optimization might be conflicting with each other, so there is no single optimal solution to a given problem. Therefore, the solutions are non-dominated "Pareto optimal", which are the trade-offs between the sub-objectives. For arbitrary given two decision vectors $\vec{x}_1$ and $\vec{x}_2$, it can be said that $\vec{x}_1$ dominates $\vec{x}_2$ (denoted as $\vec{x}_1 \prec \vec{x}_2$) if the following conditions are satisfied: 1) the solution in decision vector $\vec{x}_1$ is no worse than that of decision vector $\vec{x}_2$ in all objectives; 2) the solution in decision vector $\vec{x}_1$ is strictly better than that of $\vec{x}_2$ in at least one objective. The conditions can be described mathematically as

$$\forall i \in \{1,2,\cdots,m\}:\ f_i(\vec{x}_1) \le f_i(\vec{x}_2) \tag{5}$$

$$\exists j \in \{1,2,\cdots,m\}:\ f_j(\vec{x}_1) < f_j(\vec{x}_2) \tag{6}$$

Additionally, a solution $\vec{x}^*$ is called non-dominated solution if there does not exist another solution that dominates it. The set of the non-dominated solutions is called the Pareto front, e. g. for a minimization problem with two objectives, and the dominated and non-dominated solutions are shown by Figure 1.

The NSGA-II (Non-dominated Sorting Genetic Algorithm) is applied to solve the multi-objective optimization problem in this study. NSGA-II is one of the most popular multi-objective optimization algorithms with three special characteristics, fast non-dominated sorting approach, fast crowded distance estimation procedure, and simple crowded comparison operator. Currently, the NSGA-II algorithm is widely used in the multi-objective optimization field (Deb et al., 2002).

2.3 Approach 3: Non-dominated sorting with sub-objective constraints

Optimization results beyond the tolerable limits may appear with direct application of the multi-objective optimization algorithm. Hence, the multi-objective optimization method with constraints of sub-objectives is studied. First, the minimization optimization problem is converted into the maximization optimization problem, given as

$$\text{maximize } g(\vec{x}) = \left[g_i(\vec{x})\right]^T, i = 1,2,\cdots,m, \tag{7}$$

where the sub-objectives are defined as

$$g_i(\vec{x}) = \begin{cases} \dfrac{1}{1+f_i(\vec{x})}, & \text{if } f_i(\vec{x}) \le f_{i,0} \\ 0 & \text{else} \end{cases}. \tag{8}$$

Then, Eqs 7, 8 are implemented into the non-dominated sorting algorithm NSGA-II for the multi-objective optimization.

3 Results and discussion

3.1 The savannah reactor shielding model

The simplified Savannah reactor model is introduced to perform radiation shielding design optimization. The Savannah is a single-screw, combination passenger-cargo ship, which is powered by a nuclear reactor (Blizard et al., 1962). The Savannah reactor is of the pressurized water type, fueled with slightly enriched UO_2. The critical core is 229.2 cm long overall, with an active fuel length of 167.6 cm and an equivalent core diameter of 157.6 cm. The initial design for the Savannah reactor

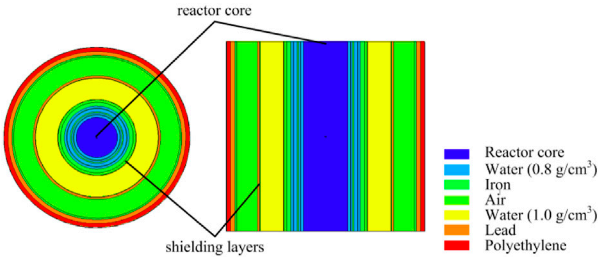

FIGURE 2
Schematic of the radial and axial cross-section of the simplified Savannah reactor shield model.

shield is a simplified shield model which consists of an annulus of light water and stainless steel contained in the shield tank surrounding the reactor. The water annulus is supplemented by lead at the shield tank outer wall. The simplified shield model of the Savannah reactor is shown in Figure 2. The visualization toolkit Vised is used to visualize the geometrical structures of the reactor shielding (X-5 Monte Carlo Team, 2003).

There are 18 shielding layers surrounding the reactor core. Thicknesses of the pressure vessel, air insulator, and containment vessel are considered to be fixed; thus, the number of the optimization parameters is 13. The initial layers of geometrical structures with different materials and the initial design parameters and ranges of the optimization parameters are listed in Table 1. Ranges of the optimization parameters are considered based on the engineering needs of the Savannah reactor (Blizard et al., 1962).

3.2 The optimization objectives

For the Savannah reactor, the purpose of optimizing is to obtain a lightweight and compact shielding structure with the radiation dose in the tally volume lower than the tolerable limit. Hence, the three optimization objectives are the shielding weight, radiation dose in the tally volume, and volume of the shielding structure, denoted as f_W, f_D, and f_V, respectively. In addition, the fast neutron flux (> 1.0 MeV) at the pressure vessel should be lower than the tolerable limit value to ensure the operation life of the reactor, so the fast neutron flux at the pressure vessel, denoted as f_4, acts as a constraint during the optimization.

The shielding weight, volume, radiation dose in the tally volume, and fast neutron flux at the pressure vessel of the initial design of the Savannah reactor perform as the tolerable limits of the sub-objectives during the optimization. The paralleling SN code *Hydra* is applied to perform the radiation transport simulation. Fixed-source calculations with one source iteration are performed in the S16-P3 approximation, where S16 indicates the flux angular discretization is 16 and P3 indicates the order of the expansion in Legendre polynomials of the scattering cross-section is 3. The BUGLE-96 (Broad User Group Library ENDF/B) cross-section library, specifically produced for LWR (Light-Water Reactor) shielding and dosimetry applications, is used in the *Hydra* calculations. BUGLE-96 is based on the ENDF/B-VI

TABLE 1 Structure of the Savannah reactor shield and the optimization parameters.

	Material	Initial values (cm)	Optimization parameter	Range (cm)
—	Reactor core	78.7	—	—
1	Water (0.8 g/cm^3)	9.5	x_0	0–20
2	Iron	2.5	x_1	0–20
3	Water (0.8 g/cm^3)	5.7	x_2	0–20
4	Iron	5.1	x_3	0–20
5	Water (0.8 g/cm^3)	11.9	x_4	0–20
6	Iron	2.5	x_5	0–20
7	Water (0.8 g/cm^3)	7.6	x_6	0–20
8	Iron (Pressure vessel)	15.2	—	—
9	Air (Insulation)	10.2	—	—
10	Fe	1.0	—	—
11	Water (1.0 g/cm^3)	83.8	x_7	50–150
12	Iron	1.5	x_8	0–20
13	Lead	7.6	x_9	0–20
14	Air (space with equipment)	274.3	x_{10}	274.32–518.16
15	Iron (containment vessel)	6.4	—	—
16	Lead	15.2	x_{11}	0–50
17	Polyethylene	15.2	x_{12}	0–50
18	Air (tally volume)	1.0	—	—

TABLE 2 Tolerable limits of the sub-objectives.

Sub-objective	$f_{W,0}$ (ton)	$f_{D,0}$ (Sv·h^{-1})	$f_{V,0}$ (m^3)	$f_{4,0}$ (n·cm^{-2}·s^{-1})
Tolerable limit (by *Hydra*)	202.9	3.8×10^{-5}	162.1	7.6×10^9
Tolerable limit (by MCNP)	—	4.1×10^{-5}	—	8.3×10^9

(Evaluated Nuclear Data File) Release 3 evaluated data and is available in the FIDO (Floating Index Data Operation) ANISN format (White et al., 1996). The MCNP code is also carried out to calculate the tolerable limits of the sub-objectives, listed in Table 2. The relative deviation between the *Hydra* code and the MCNP code for $f_{V,0}$ and $f_{4,0}$ are 8 and 8.7%, respectively, indicating that the accuracy of *Hydra* code is sufficient for optimization.

In order to keep the sub-objectives to the same scale, the sub-objectives are normalized using the following method, given by

$$f_1 = \frac{f_W}{f_{W,\max} - f_{W,\min}}$$
$$f_2 = \frac{f_D}{f_{D,\max} - f_{D,\min}}, \quad (9)$$
$$f_3 = \frac{f_V}{f_{V,\max} - f_{V,\min}}$$

where $f_{W,\max}$, $f_{W,\min}$, $f_{D,\max}$, $f_{D,\min}$, $f_{V,\max}$, and $f_{V,\min}$ are the maximum and minimum values of the shielding weight, radiation dose, and the shielding volume, respectively, among the optimization range listed in Table 1.

3.3 The optimization algorithm parameter's setting

Population size used in the optimization is 70, and the number of generations is 100. The SBX (Simulated Binary Crossover) operator is adopted with the crossover rate of 0.9. The polynomial mutation operator is used with the mutation rate of 0.2.

3.4 The optimization results

3.4.1 Optimization with two objectives

First, situations with two competing sub-objectives are studied, i. e., the shielding weight and radiation dose in the tally volume. Four cases are studied in this section. The optimization approach and objectives of each case are illustrated in Table 3. The optimized objectives (for case 1 and case 2) and the Pareto fronts (for case 3 and case 4) are illustrated in Figure 3.

TABLE 3 Optimization cases.

Case	Optimization approach	Objective
Case 1	Approach 1	Weight
Case 2	Approach 1	Radiation dose
Case 3	Approach 2	Weight and dose
Case 4	Approach 3	Weight and dose

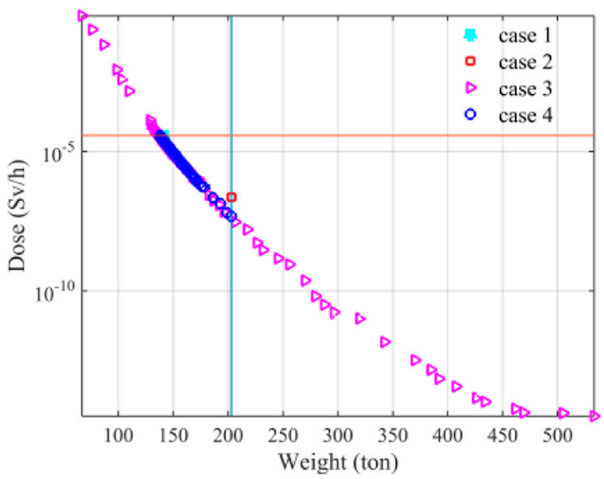

FIGURE 3
Optimized objectives and Pareto fronts of the optimization cases.

As is shown in Figure 3, the optimized objectives of case 1 and case 2 are close to the Pareto front of case 3. The Pareto front curve of case 4 overlaps with the Pareto front curve of case 3. For the optimization results of case 3, there are 35 individuals of which the sub-objectives are within the tolerable limits. However, for the optimization results of case 4, there are 70 individuals of which the sub-objectives are within the tolerable limits, indicating that more optimized individuals can be obtained by applying constraints on the sub-objectives for optimization.

The geometrical structures of the initial design and eight typical individuals picked from the optimization results of the four cases are studied and shown in Figure 4. The eight typical optimized individuals are the optimized individuals of case 1,

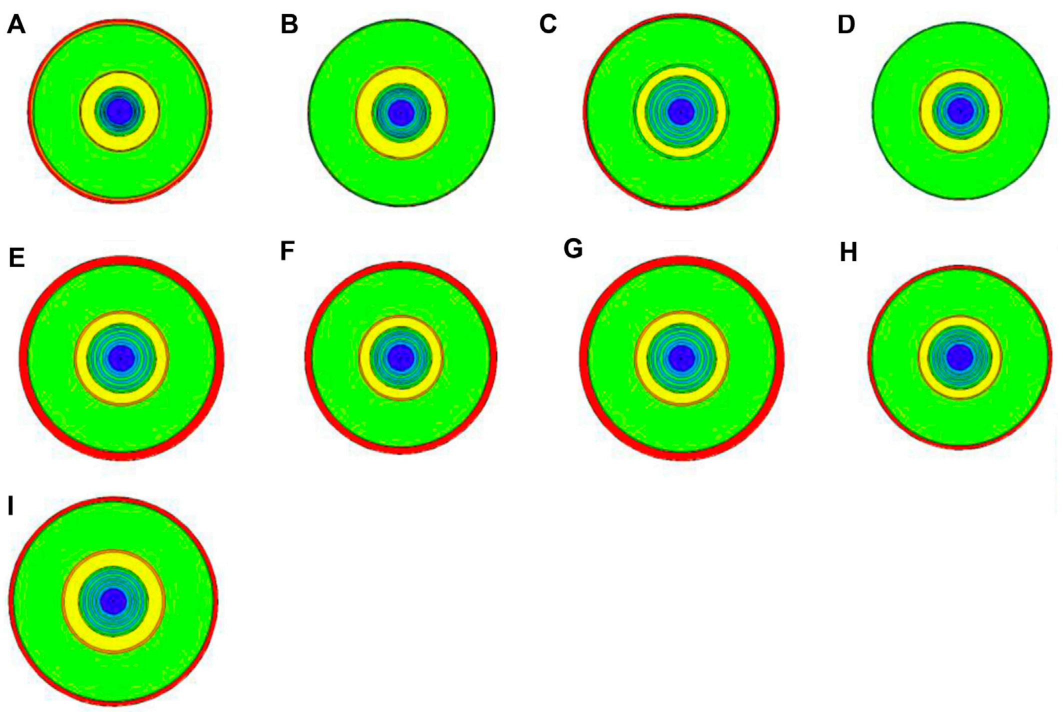

FIGURE 4
Cross-sections of the geometrical structures of the initial design and typical individuals after optimization; **(A)** initial design; **(B)** case 1; **(C)** case 2; **(D)** case 3 with minimal weight; **(E)** case 3 with minimal dose; **(F)** case 3 with minimal weight within tolerable limits; **(G)** case 3 with minimal dose within tolerable limits; **(H)** case 4 with minimal weight; and **(I)** case 4 with minimal dose.

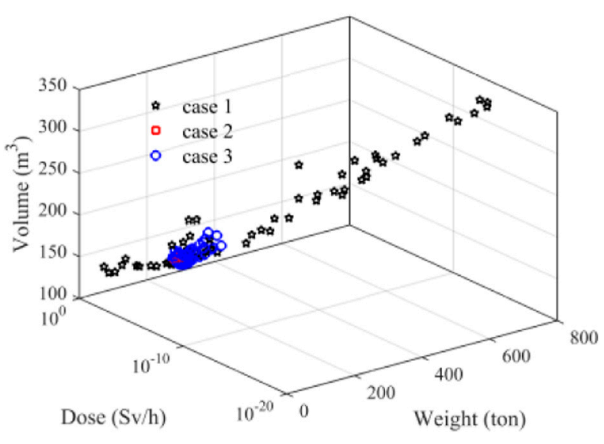

FIGURE 5
Pareto fronts of the optimization cases.

case 2, and case 3 with minimal weight, case 3 with minimal dose, case 3 with minimal weight under tolerable limits, case 3 with minimal dose under tolerable limits, case 4 with minimal weight, and case 4 with minimal dose.

TABLE 4 Sub-objectives of the initial design and typical optimized individuals.

	Weight (ton)	Dose (Sv/h)
(a)	202.9	3.8×10^{-5}
(b)	141.2	3.8×10^{-5}
(c)	202.9	2.3×10^{-7}
(d)	109.9	1.5×10^{-3}
(e)	533.2	3.2×10^{-15}
(f)	148.6	1.0×10^{-5}
(g)	196.2	6.9×10^{-8}
(h)	138.3	3.4×10^{-5}
(i)	202.8	4.6×10^{-8}

Comparing with the initial design, the optimized structures are oriented by the optimization objectives. As for the two competing sub-objectives, the optimized structure with minimal weight appears to have the maximal dose and vice versa, as shown in Figures 4D,E. The other individuals show the same pattern. The sub-objectives of the optimized individuals in Figure 4 are listed in Table 3. It can be seen that the optimization

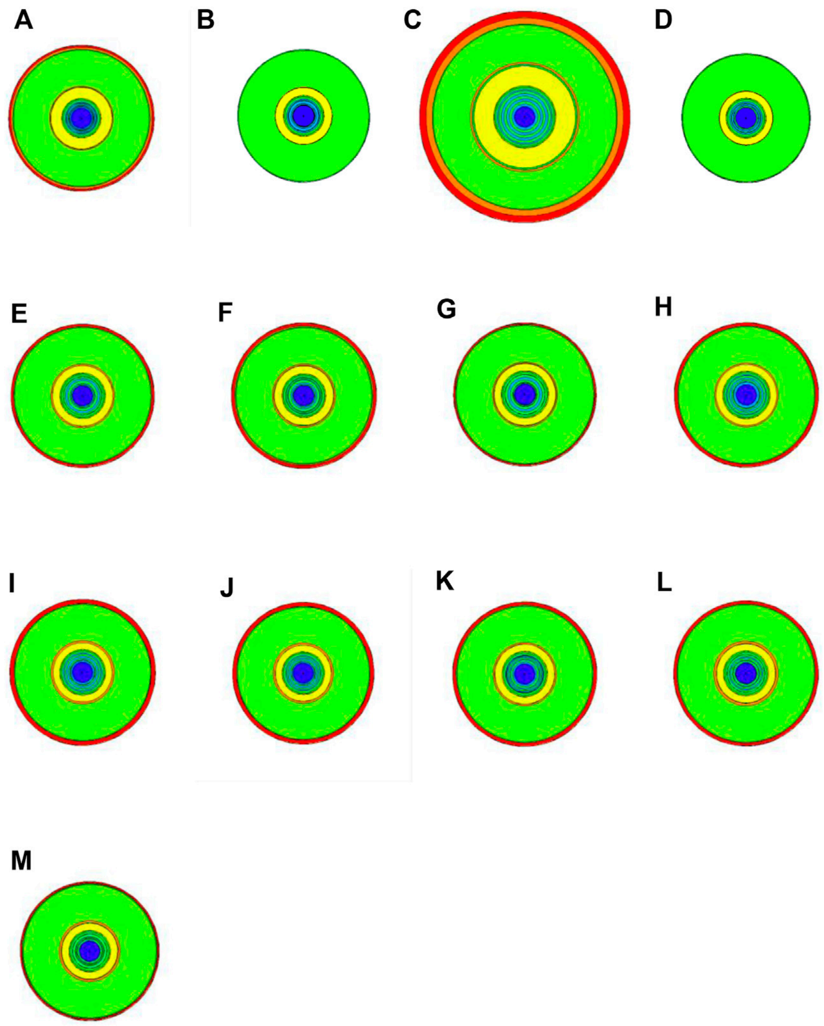

FIGURE 6
Cross-sections of the geometrical structures of the initial design and typical individuals after optimization; **(A)** initial design; **(B)** case 1 with the minimal weight; **(C)** case 1 with the minimal dose; **(D)** case 1 with the minimal volume; **(E)** case 1 with the minimal weight within the tolerable limits; **(F)** case 1 with the minimal dose within the tolerable limits; **(G)** case 1 with the minimal volume within the tolerable limits; **(H)** case 2 with minimal weight; **(I)** case 2 with minimal dose; **(J)** case 2 with minimal volume; **(K)** case 3 with minimal weight; **(L)** case 3 with minimal dose; and **(M)** case 3 with minimal volume.

result with approach 3 contains the best individuals with sub-objectives under the tolerable limits, shown (h) and (i) in Table 4. Comparing with the initial design, the optimized weight can be reduced by 31.8% (h) and the radiation dose can be reduced by ~ three orders of magnitude (i).

3.4.2 Optimization with three objectives

Optimizations with two competing sub-objectives are studied in Section 3.4.1, and the results agree well with the theoretical anticipation. In this part, optimizations with three sub-objectives are also studied. The sub-objective dose is competing with the other two sub-objectives, i e., weight and volume. The sub-objectives weight and volume are positively correlated, however not equivalent. Three cases are studied in this section. The optimization approach and limit value of the weight of the cases are illustrated in Table 5.

Pareto fronts of the three cases are shown in Figure 5.

The number of the optimized individuals of which the sub-objectives are under the tolerable limits for the three cases is 9, 13, and 27. The "relaxation" is effective for the tight limitation that generates too many lethal genes which may cause difficulty for the algorithm searching for the optimal solutions.

The geometric structures of the initial design and the typical optimized individuals are shown in Figure 6. The typical optimized individuals are as follows: case 1 with

TABLE 5 Optimization cases with three objectives.

Case	Optimization method	Limit value of weight (ton)
Case 1	Approach 2	None
Case 2	Approach 3	162.1
Case 3	Approach 3	300.0

TABLE 6 Sub-objectives of the initial design and the typical optimized individuals.

	Weight (ton)	Dose ($Sv\cdot h^{-1}$)	Volume (m^3)
(a)	202.9	3.8×10^{-5}	162.1
(b)	70.9	8.6×10^{-1}	130.2
(c)	760.7	2.7×10^{-15}	334.9
(d)	74.4	3.8×10^{-1}	124.6
(e)	146.5	2.9×10^{-5}	155.9
(f)	201.1	4.6×10^{-6}	160
(g)	148.3	3.4×10^{-5}	153.1
(h)	140.7	3.1×10^{-5}	158.1
(i)	156.7	1.1×10^{-5}	162
(j)	147.5	3.5×10^{-5}	155.7
(k)	140	3.8×10^{-5}	158.1
(l)	171.8	4.0×10^{-6}	159.2
(m)	166.6	3.8×10^{-5}	147.6

minimal weight, case 1 with minimal dose, case 1 with minimal volume, case 1 with minimal weight within the tolerable limits, case 1 with minimal dose within the tolerable limits, case 1 with minimal volume within the tolerable limits, case 2 with minimal weight, case 2 with minimal dose, case 2 with minimal volume, case 3 with minimal weight, case 3 with minimal dose, and case 3 with minimal volume.

Similar to the optimization results in Section 3.4.1, the optimized structures are oriented by the optimization objectives. As for the competing sub-objectives, i. e., weight and dose, the optimized structure with minimal weight appears to have the maximal dose and vice versa, as shown in Figures 6B,C. Also, as for the two positively correlated sub-objectives, i. e., weight and volume, the optimized structures are also positively correlated, as shown in Figures 6B,D.The other individuals show the same pattern. The sub-objectives of the initial design and the typical optimized individual are listed in Table 6. It can be seen that the optimization result with method 3 with "relaxation" contains best individuals with sub-objectives under the tolerable limits, shown as (k), (l), and (m) in Table 6. Comparing with the initial design, the optimized weight (k), the optimized radiation dose (l), and the optimized volume (m) are reduced by 31.0, 89.4, and 9.0%, respectively.

Comparing with the optimized results of Section 3.4.1, the optimized individuals with minimum weight and dose are a little higher. Increase of the sub-objectives may cause difficulty for the optimization algorithm searching for optimal solutions.

4 Conclusion

An optimization method combining the non-dominated sorting genetic algorithm with the paralleling 3-dimensional SN code is developed and applied to radiation shielding design of the Savannah reactor. Better performances of the radiation shielding structure can be obtained through optimization. For example, as for the optimization with two objectives, the optimized shielding weight and radiation dose can be reduced by 31.8% and ~3 orders of magnitude, respectively. The optimized shielding weight, radiation dose, and shielding volume of the optimization with the three objectives are reduced by 31.0, 8.4, and 9.0%, respectively. The developed method is meaningful for lightweight and compact design of nuclear reactors. However, sub-objectives that the developed method can process are too few to shielding design of some types of reactors with special purposes, so optimization design method processing many sub-objectives (~10) is to be developed in the future.

Data availability statement

The raw data supporting the conclusion of this article will be made available by the authors, without undue reservation.

Author contributions

BL designed the research and wrote the paper; YT raised valuable questions that help improving the paper; FJ performed the HYDRA calculations; GH conducted the research and performed the genetic algorithm; MY performed the MCNP calculations.

Conflict of interest

The authors declare that the research was conducted in the absence of any commercial or financial relationships that could be construed as a potential conflict of interest.

Publisher's note

All claims expressed in this article are solely those of the authors and do not necessarily represent those of their affiliated organizations, or those of the publisher, the editors, and the reviewers. Any product that may be evaluated in this article, or claim that may be made by its manufacturer, is not guaranteed or endorsed by the publisher.

References

Ahmad, S., Chang, B., Li, B., Qi, Y., and Liu, C. (2021). Mass optimization of the radiation shadow shield for space nuclear power system. *Prog. Nucl. Energy* 131 (1), 103607. doi:10.1016/j.pnucene.2020.103607

Blizard, E. P., Blosser, T. V., and Freestone, R. M. (1962). *The radiation leakage survey of the shield of the nuclear ship Savannah*. ORNL-3336. United States: Oak Ridge National Laboratory.

Cacuci, D. G. (2010). *Handbook of nuclear engineering*. Boston, MA, USA: Springer.

Cai, Y., Hu, H. S., Lu, S. Y., and Jia, Q. (2018). Optimization of radiation shielding material aiming at compactness, lightweight, and low activation for a vehicle-mounted accelerator-driven D-T neutron source. *Appl. Radiat. Isotopes* 135, 147–154. doi:10.1016/j.apradiso.2018.01.021

Chen, Z. P., Zhang, Z. Y., Xie, J. S., Guo, Q., and Yu, T. (2019). Metaheuristic optimization method for compact reactor radiation shielding design based on genetic algorithm. *Ann. Nucl. Energy* 134 (1), 318–329. doi:10.1016/j.anucene.2019.06.031

Chen, Z. P., Zhang, Z. Y., Xie, J. S., Guo, Q., Yu, T., Zhao, P., et al. (2020). Multi-objective optimization strategies for radiation shielding design with genetic algorithm. *Comput. Phys. Commun.* 260 (1), 107267. doi:10.1016/j.cpc.2020.107267

Deb, K., Pratap, A., Agarwal, S., and Meyarivan, T. (2002). A fast and elitist multi-objective genetic algorithm: NSGA-II. *IEEE Trans. Evol. Comput.* 6 (2), 182–197. doi:10.1109/4235.996017

El-Genk, M. S. (2009). Deployment history and design considerations for space reactor power systems. *Acta Astronaut.* 64 (1), 833–849. doi:10.1016/j.actaastro.2008.12.016

Ma, B. L., Song, L., Yan, M. F., Ikeda, Y., Otake, Y., and Wang, S. (2021). Multi-objective optimization shielding design for compact accelerator-driven neutron sources by application of NSGA-II and MCNP. *IEEE Trans. Nucl. Sci.* 68 (2), 110–117. doi:10.1109/tns.2020.3040500

Tunes, M. A., de Oliveira, C. R. E., and Schon, C. G. (2017). Multi-objective optimization of a compact pressurized water nuclear reactor computational model for biological shielding design using innovative materials. *Nucl. Eng. Des.* 313 (1), 20–28. doi:10.1016/j.nucengdes.2016.11.009

Wang, Y. P., Zheng, Y. Q., Xu, L. F., and Cao, L. (2020). NECP-Hydra: A high-performance parallel SN code for core-analysis and shielding calculation. *Nucl. Eng. Des.* 366 (1), 1107111–1107118. doi:10.1016/j.nucengdes.2020.110711

White, J. E., Ingersoll, D. T., and Wright, R. Q., (1996). Production and testing of the revised VITAMIN-B6 fine-group and the BUGLE-96 broad-group neutron/photon cross section libraries derived from ENDF/B-BI.3 nuclear data, NUREG/CR-6214, Revision 1, ORNL-6795/R1.

Wu, X., Yang, Y. W., Han, S., Zhao, Z., Fang, P., and Gao, Q. (2021). Multi-objective optimization method for nuclear reactor radiation shielding design based on PSO algorithm. *Ann. Nucl. Energy* 160 (1), 108404. doi:10.1016/j.anucene.2021.108404

X-5 Monte Carlo Team (2003). *MCNP-A general N-particle transport code*. New Mexico: Los Alamos National Laboratory.

Yamaji, A., and Sako, K. (1994). Shielding design to obtain compact marine reactor. *J. Nucl. Sci. Technol.* 31 (6), 510–520. doi:10.1080/18811248.1994.9735185

Zhou, M., and Sun, S. D. (1999). *Genetic algorithms: Theory and applications*. Beijing, China: National Industrial Press.

Zhuang, S. X., He, P., Sun, G. Y., Hao, L., and Wu, Y. (2019). Hybrid Monte Carlo-deterministic method for 3D neutron transport simulation based on energy region division. *Ann. Nucl. Energy* 130 (1), 271–276. doi:10.1016/j.anucene.2019.02.043